

Charge Transfer States in Stable Neutral and Oxidized Radical Adducts from Carbazole Derivatives

Lluís Fajari,[†] Robert Papoular,[‡] Marta Reig,[§] Enric Brillas,^{||} José Luis Jorda,[⊥] Oriol Vallcorba,[#] Jordi Rius,[#] Dolores Velasco,[§] and Luis Juliá^{*,†}

[†]Departament de Química Biològica i Modelització Molecular, Institut de Química Avançada de Catalunya (CSIC), Jordi Girona 18-26, 08034 Barcelona, Spain

[‡]Laboratoire Leon Brillouin, IRAMIS, CEA-Saclay, 91191 Gif-sur-Yvette, France

[§]Departament de Química Orgànica Institut de Nanociència i Nanotecnologia (IN2UB), Universitat de Barcelona, Martí Franquès 1-11, 08028 Barcelona, Spain

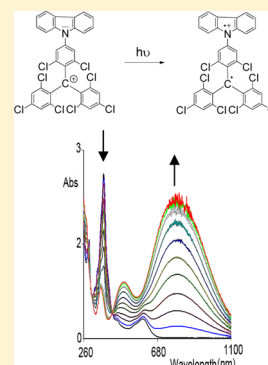
^{||}Departament de Química Física, Universitat de Barcelona, Martí Franquès 1-11, 08028 Barcelona, Spain

[⊥]Instituto de Tecnología Química (UPV-CSIC), Av. de los Naranjos s/n, 46022 Valencia, Spain

[#]Institut de Ciència de Materials (CSIC), Campus de la U.A.B., 08193 Bellaterra, Spain

Supporting Information

ABSTRACT: In this paper we report the spectral properties of the stable radical adducts 1^\bullet – 3^\bullet , which are formed by an electron donor moiety, the carbazole ring, and an electron acceptor moiety, the polychlorotriphenylmethyl radical. The molecular structure of radical adduct 1^\bullet in the crystalline state shows a torsion angle of approximately 90° between the phenyl and the carbazole rings due to steric interactions. They exhibit a charge transfer band in the visible range of the electronic spectrum. All of them are chemically oxidized with copper(II) perchlorate to the respective cation species, which show a strong charge transfer band into the near-infrared region of the spectrum. Radical adducts 1^\bullet – 3^\bullet and the corresponding stable oxidized species 1^+ – 3^+ are real organic mixed-valence compounds due to the open-shell nature of their electronic structure. Charge transfer bands of the cation species are stronger and are bathochromically shifted with respect to those of the neutral species due to the greater acceptor ability of the positively charged central carbon atom of the triphenylmethyl moiety. The cationic species 1^+ – 3^+ are diamagnetic, as shown by the absence of a signal in the EPR spectrum in acetonitrile solution at room temperature, but they show an intense and unique band in frozen solutions (183 K).



INTRODUCTION

Pure organic charge-transfer molecules are composed mainly of an electron-donor and an electron-acceptor moiety. In the charge-transfer excited state, the electron moves from the donor to the acceptor part of the molecule, and the resulting electrostatic attraction provides a stabilizing force for the molecular state. The two redox centers of the molecule, the donor and the acceptor, may be directly bonded or linked through a saturated or unsaturated bridge connecting both centers, and the energy of the excitation strongly depends on the nature and length of the bridge between them. Organic charge-transfer compounds play a significant role in the chemistry of materials and have found use as sensitizers for dye-sensitized solar cells.¹

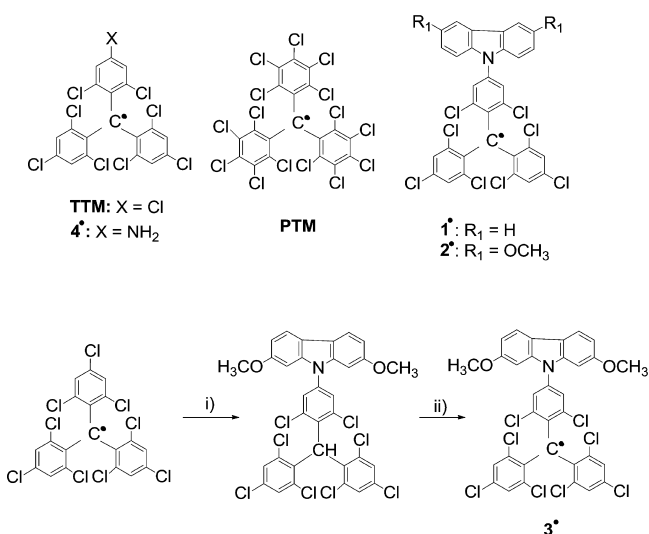
As part of our target to develop the tris(2,4,6-trichlorophenyl)methyl radical (TTM) series (Scheme 1) as electronic devices, we have been engaged in a research program to develop new stable radical adducts possessing dipolar structure built from the TTM radical, as the electron-acceptor open-shell moiety, and a heterocycle such as carbazole and indole, as the electron-donor moiety.^{2–4} All of them have shown significant physical and electrochemical properties, in addition to the intrinsic

magnetic character. Furthermore, the combination of carbazole and indole fragments with TTM has been revealed as an efficient strategy to obtain ambipolar transport properties.⁵

Now, this paper presents the photophysical properties of the radical adducts derived from carbazole, in both their neutral and oxidized states. The research work has been conducted with [4-(*N*-carbazolyl)-2,6-dichlorophenyl]bis(2,4,6-trichlorophenyl)methyl radical (1^\bullet),² [2,6-dichloro-4-(3,6-dimethoxy-*N*-carbazolyl)phenyl]bis(2,4,6-trichlorophenyl)methyl radical (2^\bullet),³ and the new radical adduct [2,6-dichloro-4-(2,7-dimethoxy-*N*-carbazolyl)phenyl]bis(2,4,6-trichlorophenyl)methyl (3^\bullet) (Scheme 1). In these compounds, the donor moiety is directly anchored on the acceptor through the nitrogen of the carbazole to the phenyl ring of the acceptor. They differ in donor strength due to the electron-donating effects of the methoxy substituent on the carbazole ring. As discussed below, all of them exhibit charge-transfer bands in both neutral (radical) and oxidized (cation) states, the bands in the cationic species being stronger and being bathochromically shifted.

Received: December 19, 2013

Published: January 27, 2014

Scheme 1. Chemical Structures of Organic Radicals TTM, PTM, 1[•], 2[•], and 4[•] and Synthesis of 3[•]


These push–pull systems are also named organic mixed valence,⁶ because they are open-shell systems. The first work reported on organic mixed-valence systems with a stable radical as electron acceptor dealt with the perchlorotriphenylmethyl radical (PTM)⁷ (Scheme 1). Since then, other systems with PTM and different electron donors have appeared in the literature.⁸

RESULTS AND DISCUSSION

Radical adducts 1[•] and 2[•] were prepared as reported by us some years ago.^{2,3} Similarly, 3[•] was obtained in a two-stage process, starting from TTM. First, TTM was treated with an excess of 2,7-dimethoxycarbazole in the presence of cesium carbonate in boiling DMF, and the resulting solid was treated with an aqueous solution of tetrabutylammonium hydroxide (TBAH) followed by oxidation with tetrachloro-*p*-benzoquinone.

The crystal structure of 1[•] was solved from synchrotron powder diffraction data measured at 100 K. An ORTEP drawing of the molecular structure is shown in Figure 1, including the atom-numbering scheme. Atomic coordinates and a selection of bond lengths and bond angles are summarized in Tables S2–S4 of the Supporting Information. This radical adduct crystallizes in the triclinic system, space group *P* $\bar{1}$. All distances and angles for the central carbon atom C(1) with aromatic carbon atoms C(2), C(8), and C(14) are in good agreement with sp² hybridization for C(1), where the spin density maximum lies. The three benzene rings are twisted around their bond with C(1) with angles displayed in Table 1. Furthermore, the torsion angle between the carbazole and the attached phenyl ring is almost perpendicular (see Table 1) to avoid interactions between hydrogen atoms. The crystal packing is controlled by Cl⋯Cl interactions (Table S5, Supporting Information). The strongest interaction (Cl33⋯Cl38) gives rise to dimeric units which propagate along *b* + *c* through the formation of slightly weaker Cl35⋯Cl36 interactions, as can be seen in Figure S3 (Supporting Information).

The UV–vis absorption spectra of radical adducts 1[•]–3[•] were recorded in the strong polar solvent acetonitrile/CHCl₃ (9/1) at concentrations of about 10^{−4} M and are shown in Figure 2. Table 2 summarizes the absorption bands and molar

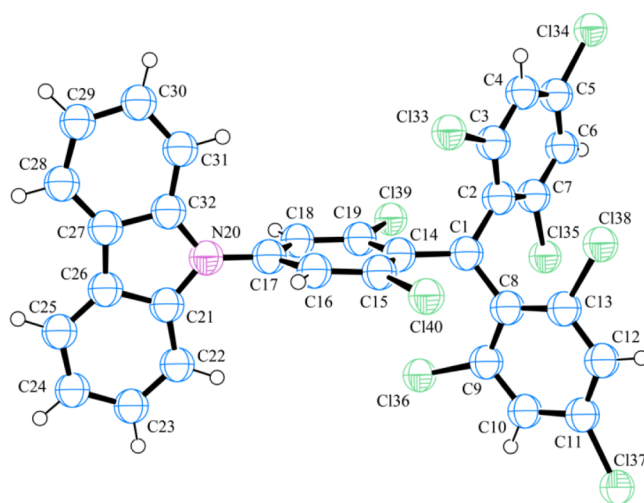


Figure 1. Perspective view of the molecular structure of the radical adduct 1[•], along with the atom numbering. Angles between planes are given in Table 1

Table 1. Selected Dihedral Angles (deg) in the Molecular Structure of Radical Adduct 1^{•a}

| P1–P4 | P2–P4 | P3–P4 | P3–P5 |
|----------|----------|---------|---------|
| 52.8(10) | 46.7(10) | 57.1(9) | 87.6(6) |

^aPlanes are defined as follows: P1, C2C3C4C5C6C7; P2, C8C9C10C11C12C13; P3, C14C15C16C17C18C19; P4, C1C2C8C14; P5, carbazole moiety.

absorptivities of all of them and the corresponding values of TTM. All of them except TTM display a band at ca. 290–307 nm assigned to the carbazole moiety. The strong band at about 370 nm and the broad and weak bands at ca. 475–555 nm in all of these radical species are characteristic of the radicals of the TTM series. Finally, the broad band at longer wavelengths (570–675 nm), strongly overlapped with the previous radical absorption band, is attributed to a charge transfer from the carbazole moiety as the electron donor to the trivalent carbon as the electron acceptor and, as said before, it is a real band from mixed-valence organic compounds since the radical adducts are open-shell systems in the ground state.⁶ The spectral region in which this charge transfer band appears is a function of the donor and/or acceptor strength of the redox centers in the molecule. In radical adducts 1[•]–3[•], this band is only slightly red-shifted with respect to the visible band of radicals, since radicals of the TTM series have a moderate electron-acceptor strength. Furthermore, the most intense and more bathochromically shifted band corresponds to the radical adduct 2[•] (λ 648 nm) due to the increased donor strength of the carbazole moiety with methoxy substitution in a position para to the nitrogen.

The emission properties of 1[•]–3[•] are summarized in Table 3, and the spectra in cyclohexane solution are shown in Figure 3. When they were excited in cyclohexane solution (λ_{exc} 450 nm), 1[•] and 3[•] showed emission in the visible region and 2[•] in the near-infrared region. The emission from 2[•] is markedly red-shifted in relation to that of 1[•] and 3[•] (100 and 90 nm, respectively), due to the relative position of the methoxy groups para to the ring nitrogen. The emission quantum yield in cyclohexane is remarkably high for 1[•] and very low for 2[•] and 3[•]. Furthermore, the quantum yield of 1[•] decreases in CHCl₃ and no fluorescence was detected for 2[•] and 3[•] in this

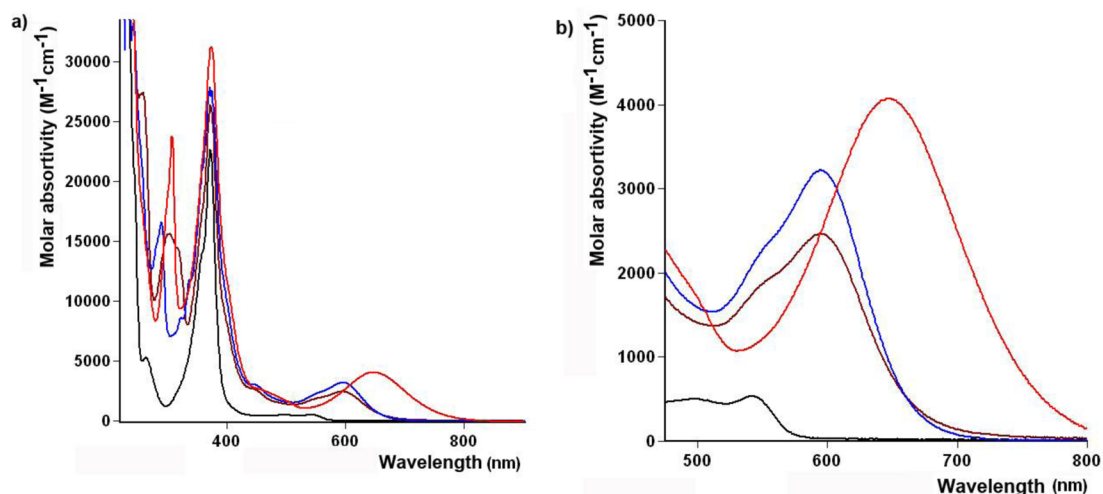


Figure 2. (a) UV-vis spectra of radical adducts 1^{\bullet} (brown), 2^{\bullet} (red), 3^{\bullet} (blue), and TTM (black) in acetonitrile/ CHCl_3 (9/1) and (b) details of the charge transfer bands.

Table 2. UV-Vis Absorption Data of Radical Adducts 1^{\bullet} – 3^{\bullet} and TTM and Their Corresponding Oxidized Species in Acetonitrile/ CHCl_3 (9/1)

| adduct | λ_{max} nm (ϵ , $\text{dm}^3 \text{mol}^{-1} \text{cm}^{-1}$) | λ_{max} nm (ϵ , $\text{dm}^3 \text{mol}^{-1} \text{cm}^{-1}$) |
|----------------------------|-----------------------------------------------------------------------------------------|-----------------------------------------------------------------------------------------|
| 1^{\bullet} ^a | 290 (16650); 374 (27620); 555 (sh) (2400); 595 (3220) | 1^+ 356 (8580); 489 (9470); 789 (23440) |
| 2^{\bullet} ^b | 307 (23770); 373 (31220); 648 (4070) | 2^+ 304 (12040); 356 (3690); 512 (6460); 860 (16440) |
| 3^{\bullet} | 303 (15630); 372 (26450); 556 (sh) (1940); 595 (2460) | 3^+ 300 (19480); 354 (7150); 492 (7110); 781 (16820) |
| TTM | 372 (22700); 497 (505); 543 (535) | |

^aValues in CHCl_3 : 291 (14400), 374 (25600); 598 (2940).⁴ ^bValues in CHCl_3 : 373 (32600); 647 (4400).³

Table 3. Emission Spectra Properties of Radical Adducts 1^{\bullet} – 3^{\bullet} and TTM

| | solvent | λ_{em} , nm | Φ_{F} ^a |
|---------------|-----------------|----------------------------|--------------------------------|
| TTM | cyclohexane | 562 | 0.008 |
| 1^{\bullet} | cyclohexane | 628 | 0.64 (0.53 ^b) |
| | CHCl_3 | 680 | 0.06 (0.04 ^b) |
| 2^{\bullet} | cyclohexane | 728 | 0.006 |
| 3^{\bullet} | cyclohexane | 638 | 0.002 |

^aRelative fluorescence quantum yields in cyclohexane and CHCl_3 were determined using tris(2,2'-bipyridyl)ruthenium(II) chloride in water as a standard after excitation at λ 450 nm. ^bReference 4a.

solvent. These results are in agreement with the process of the fluorescence quenching of donor-acceptor molecules in polar solvents, since the excess energy of the excited state is dissipated in the intramolecular electron transfer from the donor to the acceptor.^{9,10}

Cyclic voltammograms of radical adducts 1^{\bullet} – 3^{\bullet} and TTM were measured in CH_2Cl_2 solution ($\sim 10^{-3}$ M) containing TBAP (0.1 M) as supporting electrolyte on platinum wire as the working electrode and a saturated calomel electrode (SCE) as the reference electrode. All of these radical adducts exhibit a quasi-reversible redox pair (O/R) associated with their oxidation processes, which can be attributed to the removal of one electron (Table 4). Similar values of ionization potentials were obtained for all carbazole-TTM radical adducts 1^{\bullet} – 3^{\bullet}

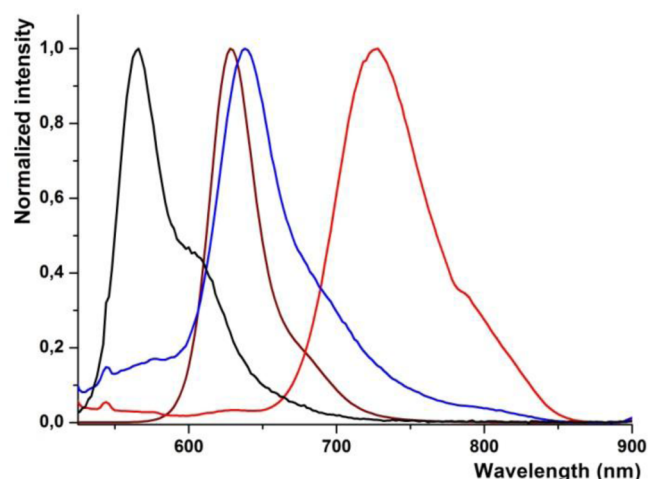


Figure 3. Normalized emission spectra of cyclohexane solutions (10^{-4} M) of radical adducts 1^{\bullet} (brown), 2^{\bullet} (red), 3^{\bullet} (blue), and TTM (black) after excitation at λ 450 nm.

Table 4. Standard Potential for the Redox Pair (O/R) Related to the Oxidation of Radical Adducts, Difference between Their Anodic (E_{p}^{a}) and Cathodic (E_{p}^{c}) Peak Potentials, and Ionization Potentials^a

| radical adduct | $E^{\circ}(\text{O/R})$, ^b V ($E_{\text{p}}^{\text{a}} - E_{\text{p}}^{\text{c}}$, mV) | E_{p}^{a} , mV | IP, ^d eV |
|----------------------------|------------------------------------------------------------------------------------------------------|--------------------------------|---------------------|
| 1^{\bullet} ^e | 1.03 (130) | 1.095 | 5.83 |
| 2^{\bullet} ^f | 0.86 (120) | 0.92 | 5.66 |
| 3^{\bullet} | 1.04 (140) | 1.11 | 5.84 |
| TTM ^e | 1.27 (100) | 1.32 | 6.07 |

^aConditions: CH_2Cl_2 solution ($\sim 10^{-3}$ M) with Bu_4NClO_4 (0.1 M) as background electrolyte on a Pt electrode at ~ 25 °C. ^bPotential values versus SCE (saturated calomel electrode). ^cValues at a scan rate of 100 mV s^{-1} . ^dIP values for radical adducts are estimated from the standard potentials of the O/R pairs, taking a value of -4.8 eV as the SCE energy level relative to the vacuum level. ^eValues taken from ref 4a. ^fValues taken from ref 3.

(5.66–5.84 eV), which are lower than that of the TTM radical (6.07 eV), where no carbazole moiety exists as an electron-donating group, the lowest one being that of 2^{\bullet} with two methoxy groups placed in positions para to the carbazole

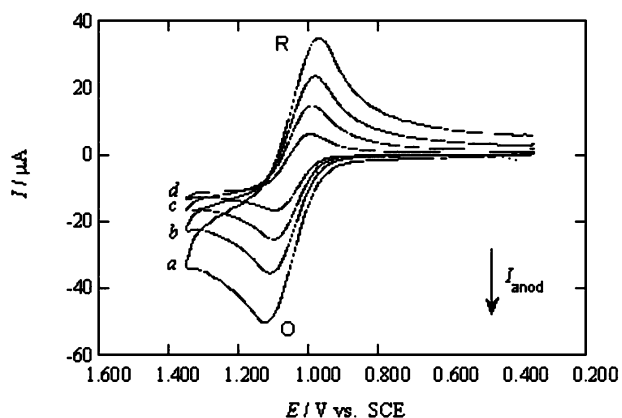
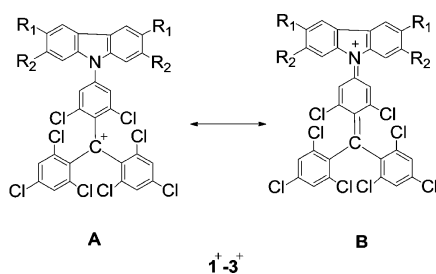


Figure 4. Cyclic voltammogram for the oxidation of radical adduct 3^\bullet ($\sim 10^{-3}$ M) in CH_2Cl_2 with 0.1 M TBAP on Pt at 25°C . The initial and final potential was 0.35 V; the reverse potential was 1.350 V. Scan rates (mV s^{-1}): (a) 200; (b) 100; (c) 50; (d) 20.

nitrogen. Figure 4 shows the cyclic voltammogram obtained for radical adduct 3^\bullet . The oxidized species are remarkably stable and do not undergo side reactions during the electrochemical process. For comparison, the cyclic voltammograms of 9-phenylcarbazole in CH_2Cl_2 under the same conditions were obtained. They displayed an irreversible oxidation peak with an anodic peak potential $E_p^a = 1.475$ V at 100 mV s^{-1} . As the potential value is much higher than the potential values (E_p^a) for radical adducts $1^\bullet-3^\bullet$ (see Table 4), we suggest that the redox pair (O/R) corresponding to the oxidation of $1^\bullet-3^\bullet$ be assigned to the equilibrium reaction involving the removal of one electron from the trivalent central carbon atom to form the stable cation. These redox processes are represented in Scheme 2, showing the additional stabilization of the cation species by the presence of the heteroatom in the para position relative to the trivalent carbon.

Scheme 2. Canonical Structures in Resonance for Cationic Species 1^+-3^+



The electronic interaction in radical adducts $1^\bullet-3^\bullet$ between the donor and the acceptor is weakened due to the noncoplanarity of the molecule, resulting from the presence of two twisted bonds between the two redox centers. One of them is located between the trivalent carbon and the phenyl ring due to the high hindrance induced by the presence of two ortho chlorines, and the other one is located between the same phenyl ring and the carbazole moiety, the torsion angle being close to 90° in the crystalline state, as shown in the molecular structure of 1^\bullet (Figure 1; see planes P3–P4 = 57° and P3–P5 = 87.6°). However, the relatively low oxidation potential values of $1^\bullet-3^\bullet$ suggest that the oxidized species, cations 1^+-3^+ , show a more planar conformation of the molecule.

Subsequently, the absorption spectra of the radical adducts $1^\bullet-3^\bullet$ after being oxidized have been studied. A few years ago, Gopidas et al. introduced copper(II) salts as good oxidizing agents of aromatic amines to generate their corresponding radical cations.^{11,12} Now, we have used a copper(II) salt to oxidize radical adducts $1^\bullet-3^\bullet$ with very interesting results. The Cu(II) salt classifies these radical species according to their reducing power. Thus, while radical adducts $1^\bullet-3^\bullet$ are oxidized by loss of an electron to the corresponding cations, radical TTM, with a higher peak potential, remains stable in the presence of Cu(II) salt.

Some of the advantages of $\text{Cu}(\text{ClO}_4)_2$ as oxidant are its solubility in acetonitrile and its easy handling. Therefore, the changes in the absorption spectra of the radical adducts $1^\bullet-3^\bullet$ have been studied according to the addition of increasing amounts of Cu(II) (Figure 5). This study has revealed that the oxidant reacts with $1^\bullet-3^\bullet$ in stoichiometric amounts; each Cu(II) ion is able to capture one electron from the radical adduct molecule and becomes a Cu(I) ion, generating the corresponding organic cation. The parent radical adducts can be reversibly recovered from the oxidant solutions by adding an excess amount of triethylamine, confirming the stability of the oxidized species and the reversibility of the chemical process. The emerging absorption bands of the oxidized species are summarized in Table 2. In all cases, when the Cu^{2+} salt concentration in the solution of the radical adduct increased, the absorption band characteristic of the radical character (λ 372–374 nm) decreased with a concurrent increase of the absorption of two new bands at λ 489–512 nm and at λ 781–860 nm, the second being stronger and broader than the first. The first new band can be ascribed to the cations 1^+-3^+ (Scheme 2), similarly to the case of the oxidation of the (4-amino-2,6-dichlorophenyl)bis(2,4,6-trichlorophenyl)methyl radical (4^\bullet) with copper(II) perchlorate, under similar conditions, giving rise to a broad band centered at λ 479 nm (see in Figure S4 (Supporting Information) the formation of cation 4^+ and the evolution graphs of UV–vis spectra on the basis of the equivalents of the salt of Cu(II)). The second and more intense band is assigned to a photoinduced electron transfer between the two redox centers of the molecule, from the carbazole nitrogen to the carbocation acceptor of the triphenylmethyl moiety, again in the same direction as in the neutral adducts. This band is remarkably shifted to the infrared in the cationic species 2^+ (λ 860 nm in front of 789 and 781 nm for 1^+ and 3^+ , respectively) due to the increased donor strength of the carbazole moiety by the presence of methoxy substituents in positions para to nitrogen. Conversely, the charge-transfer band is slightly blue-shifted in 3^+ in comparison to that of 1^+ , due to the electron-withdrawing character of the oxygen atom of the methoxy groups in positions meta to nitrogen. These observations suggest that, in the photoexcitation of the cationic species, the electron transfer band involves the nonbonded electrons on the nitrogen atom of the carbazole moiety to give diradical cation species (Scheme 3). This characteristic band is named an intervalence charge transfer (IVCT) band,⁶ as the two involved redox centers, the neutral nitrogen and the charged carbon atoms, are in different oxidation stages. The presence of isosbestic points in the measured absorption spectra when the concentration of the Cu(II) salt is varied denotes that the reaction proceeds from neutral to cationic species without multiple products.

To confirm the generation of diamagnetic species, cations 1^+-3^+ , by loss of an electron of the radical adducts $1^\bullet-3^\bullet$ in the

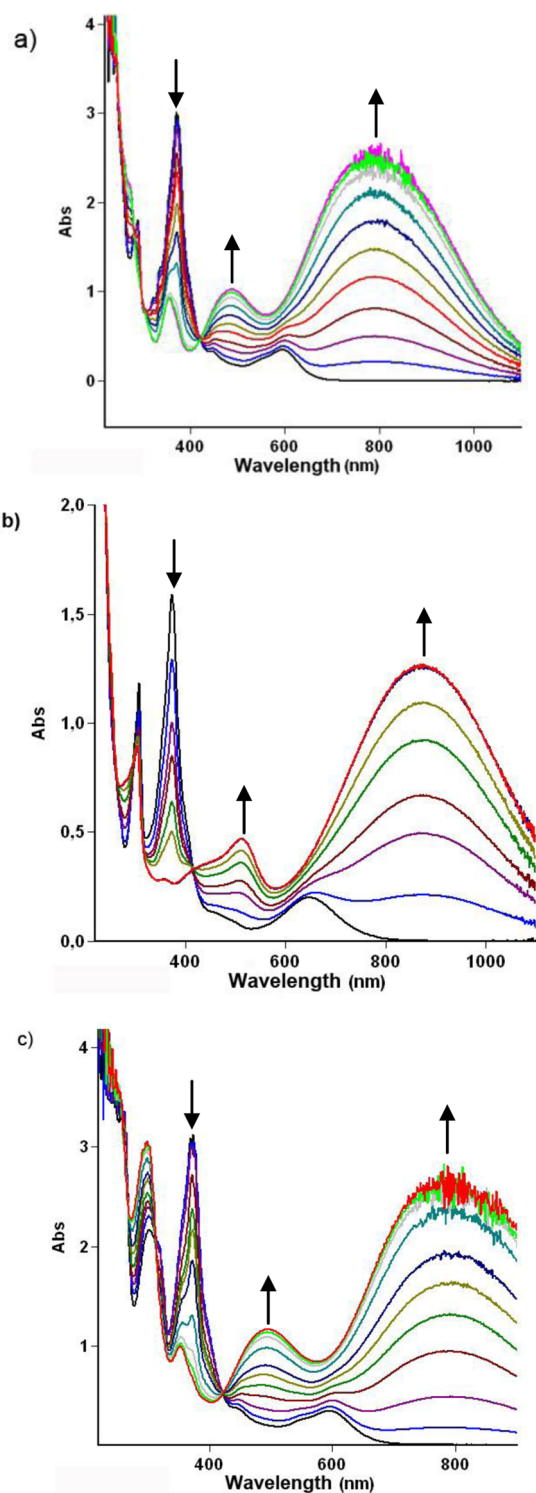
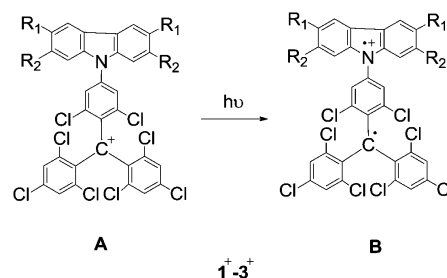


Figure 5. UV-vis spectra of radical adducts (a) 1^\bullet (0.108 mM; emerging bands $\lambda(\text{nm})$ 489, 789), (b) 2^\bullet (0.081 mM; emerging bands $\lambda(\text{nm})$ 512, 860), and (c) 3^\bullet (0.153 mM; emerging bands $\lambda(\text{nm})$ 490, 781) in $\text{CH}_3\text{CN}/\text{CHCl}_3$ (9/1) solution with different amounts of $\text{Cu}(\text{ClO}_4)_2$.

presence of copper(II) salt, their EPR spectra in acetonitrile solution with and without an excess of the oxidant $\text{Cu}(\text{ClO}_4)_2$ were registered. The spectra of the neutral form of $1^\bullet-3^\bullet$ at room temperature consisted of a broad ($\Delta H_{\text{pp}} = 4.6-4.75$ G) single line ($g = 2.0033 \pm 0.0005$). In the presence of oxidant, no signal was observed in any of them at room temperature,

Scheme 3. Photoexcitation of Cationic Species 1^+-3^+



corroborating the absence of radical species; the very weak band appearing in the spectrum of radical adduct 3^\bullet is caused by the presence of traces of unoxidized radical adduct. However, a broad and strong signal was observed for all of them in solid solution, at temperatures below the freezing point of the solvent (Figure 6).

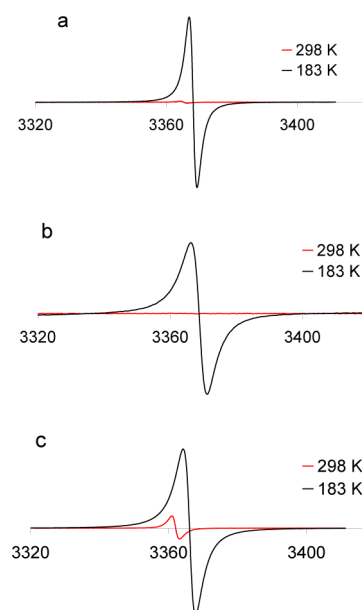


Figure 6. EPR spectra of acetonitrile solutions ($\sim 10^{-3}$ M) of the oxidized forms of radical adducts (a) 1^\bullet , (b) 2^\bullet , and (c) 3^\bullet at two temperatures.

In summary, radical adducts $1^\bullet-3^\bullet$ are formed by an electron-donor moiety, the carbazole ring, and an electron-acceptor moiety, the polychlorotriphenylmethyl radical. They exhibit a characteristic charge-transfer band of low intensity from the donor to the acceptor moiety in the visible range of the electronic spectrum. These radical adducts are chemically oxidized with copper(II) perchlorate to the respective cation species by loss of an electron from the central trivalent carbon atom. It should be mentioned that the two molecular moieties 9-phenylcarbazole and TTM remain practically stable against copper(II) perchlorate over short periods of time. The new charged species show a strong and bathochromically shifted charge transfer band into the near-infrared region of the spectrum. The most shifted band is observed in the oxidized species from 2^\bullet , when additional electron-donor substituents (methoxy groups) are placed in the carbazole ring, the donor moiety of these cationic species. These bands, both from neutral species $1^\bullet-3^\bullet$ and from cationic species 1^+-3^+ , are charge transfer bands of organic mixed-valence compounds due to the

open-shell nature of both the radical adducts 1^{\bullet} – 3^{\bullet} and their corresponding oxidized species. Charge-transfer bands of the cation species are stronger and are bathochromically shifted in comparison to those of the neutral species, due to the stronger acceptor ability of the positively charged carbon atom. The cationic species 1^+ – 3^+ may be depicted according to the Scheme 2, which is completely corroborated by the absence of signals in the EPR spectra of these cationic species in acetonitrile solution at room temperature. However, the appearance of an intense band in frozen solutions (at 183 K in Figure 6) shows the presence of radical species in the solid medium. This fact suggests that a twisted conformation (bond angle $\sim 90^\circ$ between the phenyl and carbazole rings) with a complete electron transfer from the donor to the acceptor moieties to get a diradical cation is adopted in the frozen state (structure B, Scheme 3). Predicting this new conformation in frozen acetonitrile solution is in agreement with the stable conformation assumed by the radical adduct 1^{\bullet} in the crystalline state; the bond between the phenyl and the carbazole rings undergoes a torsion angle of approximately 90° , due to steric interactions. In this regard, we have recently reported the EPR spectrum of the isolated salt $1^{\bullet}\text{SbCl}_6^-$ at 2 K, showing an intense single band ($g = 2.0030 \pm 0.0005$) and a small half-field band ($g = 4.0090 \pm 0.0005$) that confirmed the existence of a triplet state at low temperatures.⁵ The preparation and isolation of perchlorate salts of 1^{\bullet} – 3^{\bullet} and temperature-dependent EPR studies to check for the presence of triplet states at low temperatures in the twisted conformations are currently underway in our laboratories.

EXPERIMENTAL SECTION

General Procedures. IR spectra were recorded with a FT-IR spectrophotometer, electronic spectra with a single cell spectrophotometer, and the EPR spectra with a 10/12 spectrometer. DSC experiments used 40 μL closed cresol.

[2,6-Dichloro-4-(2,7-dimethoxy-*N*-carbazolyl)phenyl]bis-(2,4,6-trichlorophenyl)methyl Radical (3^{\bullet}). A mixture of 2,7-dimethoxycarbazole¹³ (1.24 g; 5.6 mmol), TTM (0.76 g; 1.37 mmol), anhydrous Cs_2CO_3 (0.76 g; 2.3 mmol), and DMF (15 mL) was stirred at reflux (2 h) under an inert atmosphere and in the dark. The resulting mixture was poured into an excess of diluted aqueous HCl acid and extracted with CHCl_3 . The organic solution was washed with water, dried over magnesium sulfate, and evaporated. The residue was chromatographed in silica gel with hexane/ CHCl_3 (1/1) to give as a second fraction, a solid (0.33 g). An aqueous solution of TBAH (1.5 M; 0.45 mL; 0.68 mmol) was added to a solution of this solid (0.33 g) in THF (10 mL) and stirred (5 h) under an inert atmosphere at room temperature, and then tetrachloro-*p*-benzoquinone (0.28 g; 1.1 mmol) was added. The solution was stirred in the dark (30 min) and evaporated to dryness, giving a residue which was filtered through silica gel with hexane/ CHCl_3 to give 3^{\bullet} (0.27 g; 27%): mp (DSC) 259 $^\circ\text{C}$ dec; IR (KBr) 3078 (w), 2925 (w), 2351 (w), 1609 (w), 1573 (w), 1522 (w), 1502 (w), 1477 (s), 1454 (s), 1429 (m), 1291 (m), 1244 (w), 1204 (s), 1165 (s), 1132 (m), 1081 (w), 1054 (m), 999 (w), 857 (w), 819 (m), 794 (m), 764 (w) cm^{-1} . Anal. Calcd for $\text{C}_{33}\text{H}_{18}\text{Cl}_8\text{NO}_2$: C, 53.3; H, 2.4; Cl, 38.1; N, 1.9. Found: C, 53.0; H, 2.4; Cl, 37.9; N, 1.7.

Cyclic Voltammetry. Cyclic voltammetry of 3^{\bullet} was carried out in a standard thermostated three-electrode cell. A platinum (Pt) disk with 0.093 cm^2 area was used as the working electrode and a Pt wire as the counter electrode. The reference electrode was a saturated calomel electrode (SCE), submerged in a salt bridge of the same electrolyte, which was separated from the test solution by a Vycor membrane. Solutions of radical adduct 3^{\bullet} ($\sim 10^{-3} \text{ M}$) in CH_2Cl_2 containing tetrabutylammonium perchlorate (0.1 M) as background electrolyte were studied. The volume of all test solutions was 50 mL. Electrochemical measurements were performed under an argon atmosphere (25 $^\circ\text{C}$)

using an Eco Chemie Autolab PGSTAT100 potentiostat–galvanostat controlled by a computer with Nova 1.5 software. Cyclic voltammograms were recorded at scan rates ranging from 20 to 200 mV s^{-1} .

Molecular and Crystal Structure of Radical Adduct 1^{\bullet} . After multiple unsuccessful attempts to grow crystals suitable for a single-crystal diffraction experiment, the crystal structure of 1^{\bullet} was solved from synchrotron powder diffraction data measured at 100 K (for details see the Supporting Information). Data indexing with the program DICVOL¹⁴ was challenging due to the presence of some impurity peaks. The final unit cell is triclinic, space group $P\bar{1}$. No phase transformation occurs between 100 K and room temperature. A similar triclinic unit cell is refined from room temperature data. For comparison purposes, both are given in Table S1 (Supporting Information). The structure solution was carried out with the direct-space method TALP¹⁵ entering as initial molecular model that derived from MM2 calculations with CS Chem3D pro. The final structure model was refined with the restrained Rietveld refinement program RIBOLS.¹⁶ Crystal data and refinement details are summarized in Table 5.

Table 5. Crystallographic Data and Structure Refinement Details of Radical Adduct 1^{\bullet} at 100 K

| | |
|--------------------------------|-------------------------------------------------|
| mol formula | $\text{C}_{31}\text{H}_{14}\text{Cl}_8\text{N}$ |
| formula wt | 684.03 |
| cryst syst | triclinic |
| space group | $P\bar{1}$ |
| a , Å | 11.8180(9) |
| b , Å | 11.8215(11) |
| c , Å | 12.7157(10) |
| α , deg | 104.206(5) |
| β , deg | 114.667(4) |
| γ , deg | 106.656(2) |
| V , Å ³ | 1404.1(2) |
| Z | 2 |
| calcd density, g/cm^3 | 1.618 |
| Rietveld refinement details | |
| no. of params | 131 |
| no. of restraints | 157 |
| R_{wp} | 0.118 |
| R_{exp} | 0.033 |
| goodness of fit (χ) | 3.604 |

ASSOCIATED CONTENT

Supporting Information

Text, figures, and tables giving synchrotron powder diffraction and X-ray crystallographic data of molecular and crystal structure of radical adduct 1^{\bullet} . This material is available free of charge via the Internet at <http://pubs.acs.org>.

AUTHOR INFORMATION

Corresponding Author

*E-mail for L.J.: ljbmoh@cid.csic.es.

Notes

The authors declare no competing financial interest.

ACKNOWLEDGMENTS

Financial support for this research from the MCI (Spain) through project CTQ2012-36074 is gratefully acknowledged. We also thank the EPR service of the Advanced Research Institute of Catalunya (CSIC) (Spain) for recording the EPR spectra and the ESRF for beamtime allocation at ID31. O.V. also thanks Consolider NANOSELECT CSD2007-00041 for a contract.

■ REFERENCES

- (1) Chochos, C. L.; Tagmatarchis, N.; GregoCriou, V. *RSC Adv.* **2013**, *3*, 7160–7181. Lin, Y.; Li, Y.; Zhan, X. *Chem. Soc. Rev.* **2012**, *41*, 4245–4272. Mishra, A.; Bauerle, M. *Angew. Chem., Int. Ed.* **2012**, *51*, 2020–2067. Walker, B.; Kim, C.; Nguyen, T.-Q. *Chem. Mater.* **2011**, *23*, 470–482. Wang, J.-L.; Zhong, C.; Tang, Z.-M.; Wu, H.; Ma, Y.; Cao, Y.; Pei, J. *Chem. Asian J.* **2010**, *5*, 105–113. Li, Y.; Guo, Q.; Li, Z.; Pei, J.; Tian, W. *Energy Environ. Sci.* **2010**, *3*, 1427–1436. Roncali, J. *Acc. Chem. Res.* **2009**, *42*, 1719–1730. Heremans, P.; Cheyns, D.; Rand, B. P. *Acc. Chem. Res.* **2009**, *42*, 1740–1747. Potscavage, W. J., Jr.; Sharma, A.; Kippelen, B. *Acc. Chem. Res.* **2009**, *42*, 1758–1767. Wu, Y.; Zhu, W. *Chem. Soc. Rev.* **2013**, *42*, 2039–2058.
- (2) Gamero, V.; Velasco, D.; Latorre, S.; López-Calahorra, F.; Brillas, E.; Juliá, L. *Tetrahedron Lett.* **2006**, *47*, 2305–2309.
- (3) Velasco, D.; Castellanos, S.; Lopez, M.; Lopez-Calahorra, F.; Brillas, E.; Julia, L. *J. Org. Chem.* **2007**, *72*, 7523–7532.
- (4) (a) Castellanos, S.; Velasco, D.; López-Calahorra, F.; Brillas, E.; Julia, L. *J. Org. Chem.* **2008**, *73*, 3759–3767. (b) López, M.; Velasco, D.; López-Calahorra, F.; Juliá, L. *Tetrahedron Lett.* **2008**, *49*, 5196–5199.
- (5) Castellanos, S.; Gaidelis, V.; Jankauskas, V.; Grazulevicius, J. V.; Brillas, E.; López-Calahorra, F.; Juliá, L.; Velasco, D. *Chem. Commun.* **2010**, *46*, 5130–5132.
- (6) Heckmann, A.; Lambert, C. *Angew. Chem., Int. Ed.* **2012**, *51*, 326–392.
- (7) Heckmann, A.; Lambert, C.; Goebel, M.; Wortmann, R. *Angew. Chem., Int. Ed.* **2004**, *43*, 5851–5856.
- (8) Heckmann, A.; Lambert, C. *J. Am. Chem. Soc.* **2007**, *129*, 5515–5527. Ratera, I.; Sporer, C.; Ruiz-Molina, D.; Ventosa, N.; Baggerman, J.; Brouwer, A. M.; Rovira, C.; Veciana, J. *J. Am. Chem. Soc.* **2007**, *129*, 6117–6129. Heckmann, A.; Diimmler, S.; Pauli, J.; Margraf, M.; Köhler, J.; Stich, D.; Lambert, C.; Fischer, I.; Resch-Genger, U. *J. Phys. Chem. C* **2009**, *113*, 20958–20966. Guasch, J.; Grisanti, L.; Lloveras, V.; Vidal-Gancedo, J.; Souto, M.; Morales, D. C.; Vilaseca, M.; Sissa, C.; Painelli, A.; Ratera, I.; Rovira, C.; Veciana, J. *Angew. Chem., Int. Ed.* **2012**, *51*, 11024–11028. Guasch, J.; Grisanti, L.; Jung, S.; Morales, D.; D'Avino, G.; Souto, M.; Fontrodona, X.; Painelli, A.; Renz, F.; Ratera, I.; Veciana, J. *Chem. Mater.* **2013**, *25*, 808–814.
- (9) Leroy-Lhez, S.; Perrin, L.; Baffreau, J.; Hudhomme, P. C. R. *Chim.* **2006**, *9*, 240–246.
- (10) Jenekhe, S. A.; Lu, L.; Alam, M. M. *Macromolecules* **2001**, *34*, 7315–7324.
- (11) Sumalekshmy, S.; Gopidas, K. R. *Chem. Phys. Lett.* **2005**, *413*, 294–299. Sreenath, K.; Suneesh, C. V.; Ratheesh Kumar, V. K.; Gopidas, K. R. *J. Org. Chem.* **2008**, *73*, 3245–3251. Sreenath, K.; Thomas, T. G.; Gopidas, K. R. *Org. Lett.* **2011**, *13*, 1134–1137.
- (12) Chang, C.-C.; Yueh, H.; Chen, C.-T. *Org. Lett.* **2011**, *13*, 2702–2705.
- (13) Morin, J. F.; Leclerc, M. *Macromolecules* **2001**, *34*, 4680–4682. Hsieh, R. B.; Litt, M. H. *Macromolecules* **1985**, *18*, 1388–1394.
- (14) Vallcorba, O.; Rius, J.; Frontera, C.; Peral, I.; Miravittles, C. J. *Appl. Crystallogr.* **2012**, *45*, 844–848.
- (15) Vallcorba, O.; Rius, J.; Frontera, C.; Miravittles, C. J. *Appl. Crystallogr.* **2012**, *45*, 1270–1277.
- (16) Rius, J. *RIBOLS18: A computer program for least-squares refinement from powder diffraction data*; Institut de Ciència de Materials de Barcelona (CSIC), Barcelona, Spain, 2009.